Reactive Crystallization of Paracetamol in a Continuous Oscillatory Baffled Reactor

Meifen Jiang and Xiong-Wei Ni[*]

EPSRC Centre for Continuous Manufacturing and Crystallization (CMAC), Centre for Oscillatory Baffled Applications (COBRA), School of Engineering and Physical Sciences, Heriot-Watt University, Edinburgh, EH14 4AS, U.K.

[*] the corresponding author, tel: 00441314513781, email: x.ni@hw.ac.uk

Abstract:

In this paper, we report, for the first time, a reactive seeded cooling crystallization of paracetamol successfully performed in a continuous oscillatory baffled reactor (COBR). The synthesis of acetaminophen took place in the first part of the COBR, generated the solvent for crystallization via a specific ratio of starting materials. Seeded cooling crystallization was immediately commenced after the completion of reaction in the second part of the COBR. We investigated the seeding strategy of three seed masses (10, 15, and 20 %) at a fixed size in this work, enabling smooth and encrustation free runs. We also estimated agglomeration by comparing the ideal to actual normalized product/seed sizes, which was confirmed by SEM images. The effect of mixing intensity on crystal properties was reported. Samples at two ports of a known distance apart along the COBR enabled the study of steady states of paracetamol concentration and crystal mean size in both temporal and spatial domains, as well as the determination of the local, in turn, the overall growth rate. Form I paracetamol particles were consistently produced with an averaged purity of 99.96 %.

Keywords: continuous reactive crystallization; mixing intensity; seeding load; steady state of concentration; steady state of crystal size, crystal growth rate; purity

1 Introduction

In industrial batch crystallization, we face the century old chemical engineering problem, i.e. mixing gets worse with increasing scales. What one has obtained in labs cannot be duplicated in production. The ability of providing a consistent mixing environment and superior heat/mass transfer for flow substances[1, 2] at all scales by continuous oscillatory baffled reactors/crystallizers (COBR/COBC) can bridge the gap, with an additional advantage of implementing online process analytical technologies (PAT)[3] anywhere along the length of COBR/COBC. This delivers consistent crystal properties and efficient process time, e.g. a 9 h and 40 min batch crystallization was achieved in 12 min in a COBC[4]. A seeded cooling crystallization of β-L-glutamic acid was successfully operated by Briggs et al.[5] in a DN15 (15 mm diameter) COBC. The steady state was achieved constantly after 2 residence times and remained for at least 10 hours, producing crystals of desirable polymorph and purity. In additional to cooling crystallization, anti-solvent[6] and co-crystal crystallisation[7] were also carried out in COBC. However, few study has been published in continuous reactive seeded crystallization, which is the focus of this work.

Paracetamol (acetaminophen) is a widely used analgesic drug in the world today. Since it was first synthesized by Morse in 1878,[8] the method of paracetamol production has gone through changes in order to enhance the productivity and product property, e.g. acetaminophen can be synthesized from 4- hydroxyacetophenone,[9-11] nitrobenzene,[12-16] 4-nitrophenol[17-19] and 4-amniophenol.[20, 21] The one-step acylation of 4-aminophenol has increasingly attracted attentions due to its simple operating conditions,[22-24] paracetamol crystals are normally separated and purified via a recrystallization process.[20, 21] Extensive work for recrystallization of paracetamol has previously been reported using cooling[25-33] and anti-solvent means.[34-42] Once again few literature can be seen for reactive crystallization in a continuous process, the closest one is the work by Agnew et al.[43, 44] who reported a selective access to produce metastable solid form of paracetamol in a COBR by adding metacetamol as a template molecule. In this work, paracetamol synthesis followed by seeded cooling crystallization were, for the first time, investigated in a COBR under different operating conditions.

2 Experimental set up and procedures

2.1 Chemicals and analytical methods

Materials

4-Aminophenmol (4-AP) (Sigma Aldrich UK Ltd.; purity, $\geq$ 99 %; MW, 109.13 g mol^{-1}) was sourced in the form of light brown crystalline powder. Paracetamol (PARA) (GlaxoSmithKline Pharmaceutical Company; purity, 99.8 %; MW, 151.16 g mol^{-1}) was purchased for the purpose of calibration of HPLC device and polymorph analysis. Acetic anhydride (AA) (purity, 99+ % pure; MW, 102.09 g mol^{-1}) and methanol (purity, HPLC grade; MW, 32.04 g mol^{-1}) were obtained from Chemistry Store at Heriot-Watt University. Distilled water (MW, 18.02 g mol^{-1}) was obtained using a water purification device from Triple Red Limited, UK.
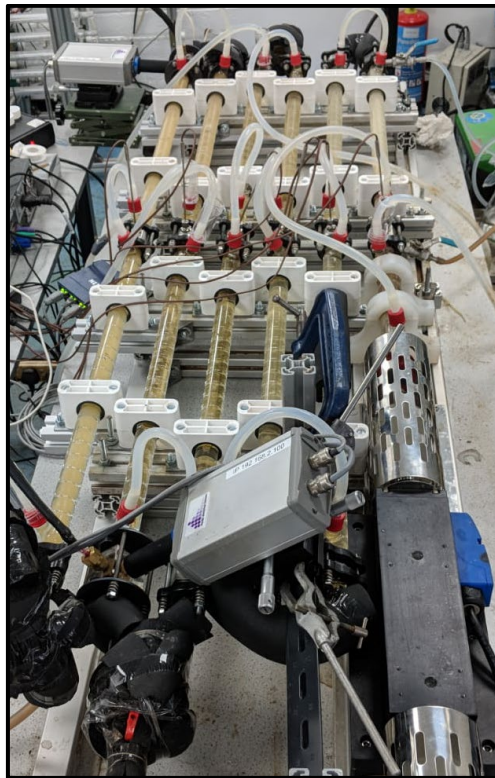
Characterization

The concentration of paracetamol from samples taken during reactive crystallization was analyzed by the Agilent1100 Series HPLC System with the column being a reverse phase ZORBAX SB-C8 (4.6×150 mm; 5 μm packing). The UV detector was set at 243 nm and the mobile phase running throughout the system was a mixture of methanol and water with a mass ratio of 1:3. Crystal size distributions were obtained via Mastersizer measurements; morphologies of crystals by a Leica ATC 2000 Trinocular Microscope, crystal surface properties by scanning electron microscope (SEM) and crystal polymorphism by Powder X-ray diffraction (PXRD).

2.2 Equipment

The reactive seeded cooling crystallization of paracetamol was carried out in a DN15 (15 mm diameter) COBR horizontally orientated, Figure 1 shows the geometrical set-up. The DN15 COBR consisted of 11 jacketed baffled straight tubes and 6 non-jacketed bends wrapped with thermos-sleeves to reduce heat loss. The total length and the volume of the COBR were 9.5 m and 1.68 L respectively. A linear motor with a control box was utilized to provide oscillation at various frequencies and amplitudes.

Peristaltic pumps (Watson Marlow 520S) were used to feed reactants and seeds from their respective stirred tanks. Water was circulated through the jackets of the COBR at preset temperatures by 3 water baths (GP 200) in order to establish three temperature zones (showing as different colours and line widths in Figure 2) for reaction and crystallization. Six

thermocouples (T1 – T6 in Figure 2) were employed to record the temperature profiles of the operation. The temperature of seed suspension was controlled and maintained by a separate water bath to achieve the required supersaturation. The tubing connecting the seed suspension with the COBR was properly insulated to ensure the correct seeding temperature. During operation, samples were taken at 3 sample points (see Figure 2) at regular times where sample point 1 was located at the end of reaction to monitor and confirm the completion of the reaction, points 2 and 3 were located in the crystallization section for the characterization of crystals.
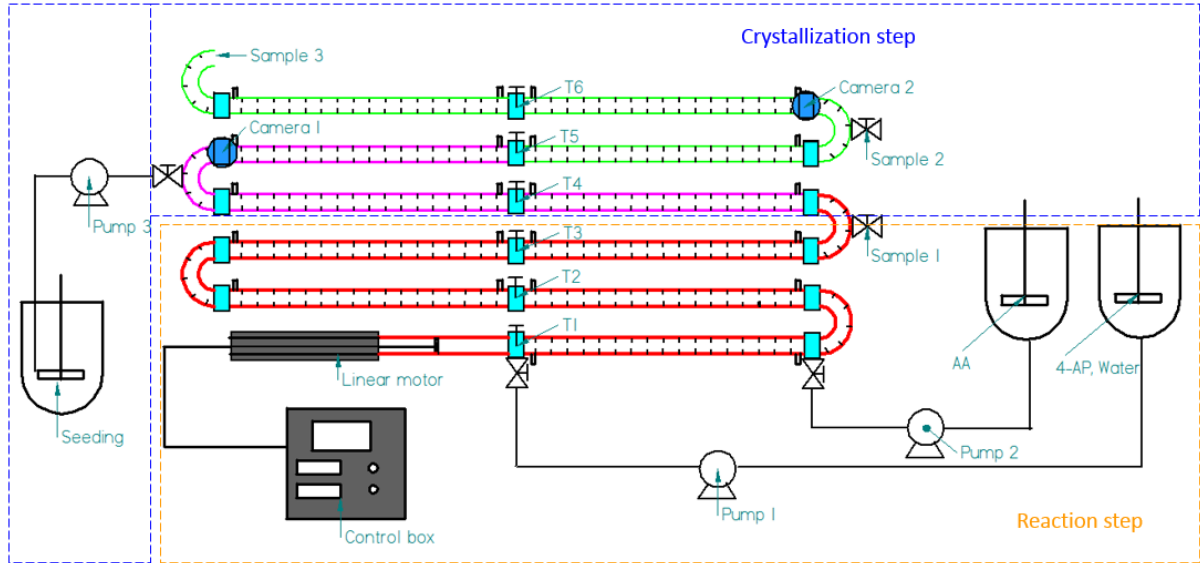

Figure 1. A photo showing the set-up of COBR

Figure 2. Schematic of the COBR platform for the reactive seeded cooling crystallization of paracetamol

Generally, the mixing performance in COBR can be characterized by three dimensionless groups: the oscillatory Reynolds number (Re_0) , the Strouhal number (St) and the net flow Reynold number (Re_n) which are defined by the following equations:[45, 46]

$$Re_0 = \frac{x_0 \omega D}{\mu} \tag{1}$$

$$St = \frac{D}{4\pi x_0} \tag{2}$$

$$Re_n = \frac{\rho u D}{\mu} \tag{3}$$

where x_0 is the oscillation amplitude from centre to peak (m), $\omega (= 2\pi f)$ the angular frequency (rad s^{-1}), f the linear frequency (Hz), D diameter of column (m) and μ kinetic viscosity of the fluid (m^2 s^{-1}), ρ the fluid density (kg m^{-3}) and u the mean velocity (m s^{-1}). The oscillatory Reynolds number is to measure the oscillation intensity, and the Strouhal number represents the ratio of column diameter to amplitude of oscillation, which determines the length of eddy

propagation. To maximize the mixing effect, the value of Re_0 should be higher than that of Re_n, the ratio of which is defined by Eq. (4) relating the oscillatory to the net flow velocity:[47]

$$\Psi = \frac{Re_0}{Re_n} \qquad (4)$$

The recommended oscillatory flow conditions include $Re_0 \geq 100$, St ≤ 0.5, $Re_n \geq 50$ and the velocity ratio Ψ in the range of 2 - 10^3.

2.3 Procedures

Paracetamol was produced by reacting 4-aminophenol and acetic anhydride, acetic acid was a side product when water reacted with the excessive acetic anhydride. At the start, the premixed 4-aminophenol and water from feed tank 1 was pumped through the COBR by pump 1 (Figure 2) at a high flow rate in order to get rid of any bubbles. Once degas has been done, the flow rate was reduced to an operational rate (Table 1) and oscillation was switched on, while the circulation continued. The purpose of circulating the mixture was to establish the three temperature zones shown in Figure 2. Once the temperature zones have successfully been set-up, acetic anhydride from feed tank 2 was introduced at a specific flow rate by pump 2 into the COBR where the temperature in this section of COBR was now at 75 °C. The reaction proceeded when the reactants were mixed and dissolved at the 1st bend and 2nd straight tube of COBR. Crystallization took place after the completion of the reaction, seed solution was fed into the COBR by pump 3 at a preset rate and at 50 ºC just before the reacted mixture has reached the seeding point. The outlet of the crystallization was collected in a product tank (not shown in Figure 2).

The shut-down procedures involve replacing the reactant feeds by water; stopping the seed pump before water has reached the seeding point; increasing the temperature of the whole COBR to 70 ºC that dissolves any residues in the system. After a certain time, the flow rate of water was increased and the temperature control switched off, COBR returned to room temperature and ready for next run. The operation conditions tested in this work are summarized in Table 1.

Table 1. COBR operation parameters

AA flow ($g \min^{-1}$)	4-AP/H_2O flow ($g \min^{-1}$)	Main flow ($g \min^{-1}$)	Seed flow ($g \min^{-1}$)	Residence time (min)
4	36	40	10	40

Sample preparation. Solution samples were taken at regular time intervals using a pipette with an accurate volume of 0.40 ml; and were quenched and diluted 100 times with the mobile phase solution (methanol:water = 1:3). Solid samples were collected by a syringe and immediately filtered, washed, then dried in an oven at 40 ºC for overnight. Dried particles were then moved to a desiccator to cool down and weighted until constant mass.

Seed preparation. Seeds were prepared using a blender and the mean size of seed crystals was measured by Mastersizer as 92.3 µm (Figure 3).
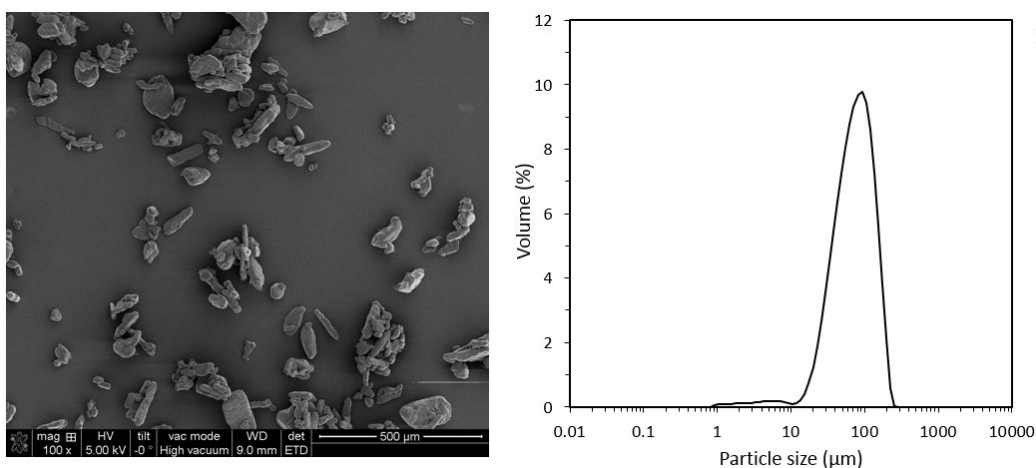

Figure 3. Particles size distribution of seed crystals

The determination of seed mass and the effect of seed mass on the sizes of final crystals are discussed later in details.

Supersaturation (S). In this work, the level of supersaturation is expressed in terms of the supersaturation ratio (S) defined as

$$S = \frac{c}{c^\star} \qquad (5)$$

where c is paracetamol concentration in solution, c* is equilibrium concentration in solution.

Operation conditions. A series of experiments from COBR-1 to COBR-6 were carried out in the COBR for the reactive seeded cooling crystallization of paracetamol. Each of the conditions was repeated 3 times for reproducibility. Table 2 summarizes the conditions.

Table 2. COBR operational conditions

| Expt. | Runs | Frequency, f (Hz) | Amplitude, $2x_0$ (mm) | R_{eo} | R_{en} | | S_t |
					Reaction	Crystallization	
	1	1	26	1225	57	71	0.09
COBR-1	2	1	26	1225	57	71	0.09
	3	1	26	1225	57	71	0.09
	1	1	30	1413	57	71	0.08
COBR-2	2	1	30	1413	57	71	0.08
	3	1	30	1413	57	71	0.08
	1	1	35	1649	57	71	0.07
COBR-3	2	1	35	1649	57	71	0.07
	3	1	35	1649	57	71	0.07
	1	0.7	30	989	57	71	0.08
COBR-4	2	0.7	30	989	57	71	0.08
	3	0.7	30	989	57	71	0.08
	1	1.2	30	1696	57	71	0.08
COBR-5	2	1.2	30	1696	57	71	0.08
	3	1.2	30	1696	57	71	0.08
	1	1.5	30	2120	57	71	0.08
COBR-6	2	1.5	30	2120	57	71	0.08
	3	1.5	30	2120	57	71	0.08

3 Results and discussion

3.1 The reaction zone

The reaction was started once the two feeds of the reactants were met in the first straight tube as shown in Figure 2; was completed just before the sample point 1 where the temperature of the reaction zone (marked in thick red line in Figure 2) was maintained at 75 ºC. The solvent for the subsequent crystallization was a mixture of acetic acid and water with an Acid: H_2O ratio of 1:9. The amounts of reactants (4-AP and AA) required to deliver the above ratio were back calculated according to the reaction stoichiometry and solubility profile;[48, 49] their flow rates were subsequently determined to ensure a required residence time of 40 mins for both reaction and crystallization. More details on calculations of the concentrations of starting materials and flow rates can be found elsewhere.[48] HPLC analysis for samples taken at the sample point 1 have confirmed that the reaction was completed, the concentration of paracetamol was approximately stable (see Figure 7) where no peak for reactants was seen in the chromatogram (see Supporting Information), i.e. about 100% of conversion was obtained.

3.2 Effect of seed loading

For successful crystallizations in COBR, correct seeding structure is one of the most important and useful methods for preventing uncontrolled nucleation and the subsequent encrustation from taking place and for focusing growth on seed crystals. [5, 50, 51] Such a structure involves a correct combination of both seed size and seed loading. Seed size is fixed in this work, as shown earlier.

A great amount of work on seeding has been carried out in batch processes,[52-54] the methodology of which could be applied to continuous crystallization. The seed loading, C_{seed} (%), is defined by Eq. (6) as the ratio of the mass of seed, W_{seed} (g), over the maximum theoretical yield, W_{theo} (g): [53, 55]

$$C_{seed} = \frac{W_{seed}}{W_{theo}} \tag{6}$$

where W_{theo} can be calculated from the solubility data. For an un-agglomerated growth only model, nucleation is totally suppressed by seeds, there is neither agglomeration nor breakage in crystals, in addition crystal shape does not change during the entire process. Based on these assumptions, the number of seed crystals (N) can be assumed to be conserved and the crystal morphology (represented by the shape factor constant, F) does not change. Given crystals with a characteristic size of S_s (µm) for seeds and S_{ip} (µm) for the ideal product crystals, the ratio of the final mass of crystals to the mass of seeds becomes:

$$\frac{W_f}{W_{seed}} = \frac{FN\rho_s S_{ip}^3}{FN\rho_s S_s^3} = \left(\frac{S_{ip}}{S_s}\right)^3 \tag{7}$$

where ρ_s is the density of solid crystal (g ml^{-1}). The final mass of product crystals, W_f (g), is a sum of the seed mass, W_{seed} (g), and the theoretical yield, W_{theo} (g) as:

$$W_f = W_{seed} + W_{theo} \tag{8}$$

Rearrangement and substitution of Eq. (6) and Eq. (8) into Eq. (7) yields:

$$\frac{W_f}{W_{seed}} = \frac{W_{theo}C_{seed} + W_{theo}}{W_{theo}C_{seed}} = \frac{1 + C_{seed}}{C_{seed}} \tag{9}$$

By equating and rearranging equations (7) and (9), we have:

$$\frac{S_{ip}}{S_s} = \left(\frac{1 + C_{seed}}{C_{seed}}\right)^{1/3} \tag{10}$$

As a result of Eq. (10), the ideal characteristic size of the product crystals, S_{ip} (µm) can be calculated when the mean size of seed crystals S_s (µm), and the seed loading, C_{seed} (%), are known. The relationship of the ideal normalized product size (S_{ip}/S_s) can graphically be represented as a function of the seed loading/mass, as shown in Figure 4.

The solid line in the seed response curve represents the effect of seed loading on the normalized product size; a decrease in the normalized product size is seen with increased seed loading. This is because the theoretical mass of crystals produced could consist of either numerous small crystals or fewer large ones, each seed crystal grows to a smaller final size

than if there were fewer seeds at the same supersaturation, thus the increase of the seed loading in Figure 4 leads to the increase of the number of crystals. This trend was also reported for adipic acid – water systems, [54] potassium alum – water systems[53] and ammonium alminium sulphate –water systems[52] in a batch stirred tank crystallizer (STC).

The seed response graph is also a very useful means for assessing seeding strategy, as the seed response curve itself represents the growth-dominated mechanism. Above the curve is associated with normalized product sizes being larger than the ideal values, in order to maintain such crystal growth this region is facilitated by non-encrustation; below the curve is the area where the final normalized product sizes are smaller than S_{ip}/S_s , two phenomena can contribute to this, either the occurrence of primary nucleation leads to massive small crystals without control or insufficient seed crystal surfaces for the solute material to grow on, solute molecules move to the reactor walls, leading to severe encrustation and blockage when seeds of larger sizes are combined with smaller seed loading. [56] To investigate the effect of seed loading on the final crystal products in this work, three runs at different seed loadings (10, 15 and 20 w/w %) were utilized in this work at a fixed seed size. The normalized actual product sizes (S_p/S_s) are the diamond symbols in Figure 4, where S_p refers to the actual size of final products (average of 5 measurements).
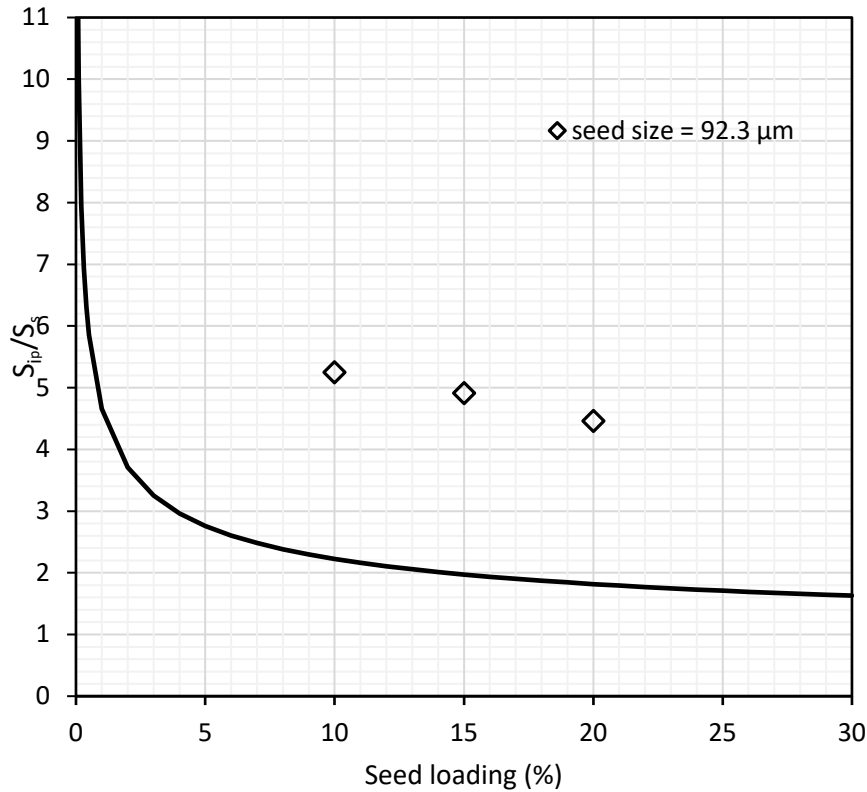
Figure 4. Seed response curve and actual product/seed ratios in COBR with a mean seed size of 92.3 μm <mark>with different seed loadings</mark>

When the seeding load increased from 10 % to 20 % in the continuous operation, the sizes of final products were 485, 453 and 412 μm respectively, giving the values of S_p/S_s of 5.25, 4.91.and 4.46, showing in the region above the seed response curve (Figure 4). Based on the above, seed loading of 15% was selected for experiments in this work. Accordingly, neither encrustation nor blockage was observed in the COBR for over 6 residence times that were the longest running time undertaken in this work.

The practical means of calculating seed mass is as follows. The theoretical solid mass concentration was 34.73 g kg^{-1} in this work when the temperature decreased from 75 ºC to 35 ºC, according to the solubility data. [48] Combining with the flow rate data in Table 1, the value of W_{theo} was calculated as 1.389 g min^{-1} by Eq. (11). Consequently, the solid concentration for seeding solution was 20.84 g kg^{-1}. To prepare this, 57.95 g paracetamol solid was added into 1 kg solvent (Acid: H_2O = 1:9 w/w) as the solubility of paracetamol was 37.11 g kg^{-1} at 50 ºC. [48]

$$C_{seed} = \frac{\text{seed concentration} \times F_{seed}}{\text{crystal products mass concentraton} \times F_{main}} \times 100\ \% \tag{11}$$

where F_{seed} (g min^{-1}) and F_{main} (g min^{-1}) are the flow rates of the seed suspension and the solution, respectively.

The fact that the actual product crystal sizes are larger than that predicted by the un-agglomerated growth model in Figure 4 suggests the existence of agglomeration, although the degree of agglomeration is difficult to estimate, as this would require data of breakage of crystals as well as crystal shape. Nevertheless, the agglomeration is confirmed by macroscopic and SEM images in Figures 7 & 10. Briggs et al.[5] reported similar results in seeded crystallizations of β-L-glutamic acid in a COBR, indicating that the decrease of the number of seed crystals was caused by agglomeration among seed crystals.

3.3 Metastable zone width and operational path

Figure 5 shows the measured paracetamol concentrations at sample point 1 (after the reaction) and 3 (at the end of crystallization) superimposed with solubility and metastable zone width obtained previously.[48, 49] We see that the solution was supersaturated post reaction at the sample point 1 at 75 ºC, the solution concentration decreased after the seeded crystallization, all within the metastable zone and close to the solubility curve. The three data points at each of the sampling locations were obtained at a fixed oscillation frequency, but different amplitudes. We see that the higher the oscillation amplitude, the lower the solution concentration, in turn the higher supersaturation for nucleation and crystal growth. This is expected as an increased mixing enhances energy dissipation and turbulence in the system,[57, 58] a solution of which is closer to its solubility curve.[51]
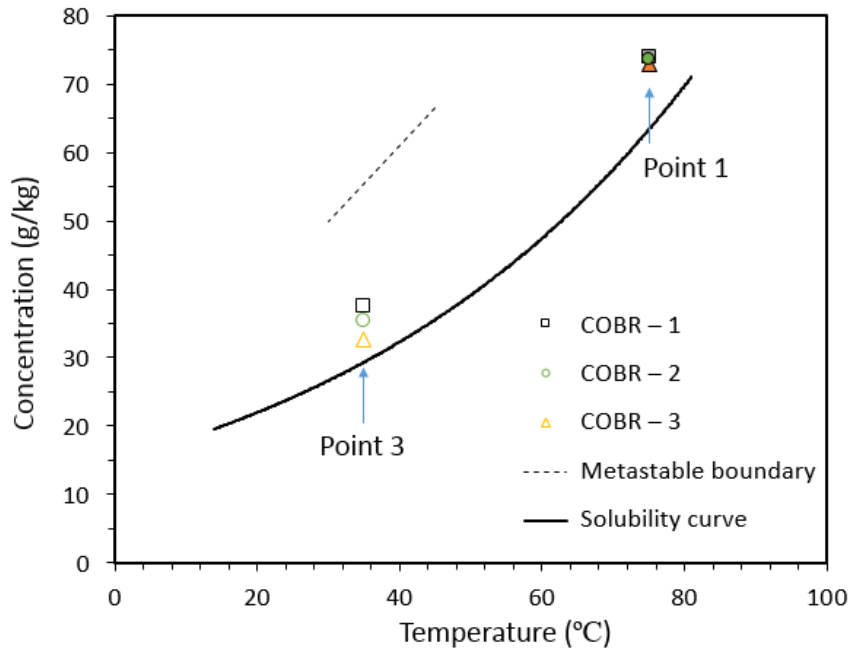
Figure 5. Data on metastable zones and supersaturation from COBR-1 to COBR-3.
Solubility, metastable zone and crystallisation path measurened gravimentrically[48] in a solvent ratio of Acid : H_2O = 1:9[49] Open symbols – concentrations after crystallisation. Close symbols – concentrations just post reaction

The data of runs COBR 4 – 6 (Table 2) were obtained at a fixed oscillation amplitude but varying frequencies. Figure 6 illustrates the effect of oscillatory Reynolds number on the average size of crystal products; particle size decreased from 527 μm to about 364 μm for Re_0 from 989 to 2120. The trend of this work agrees with that by Lawton et al.[4] where oscillation frequency/amplitude had a similar effect on crystal size distributions.[59] The shape of final crystals in this work were of column/plate like.
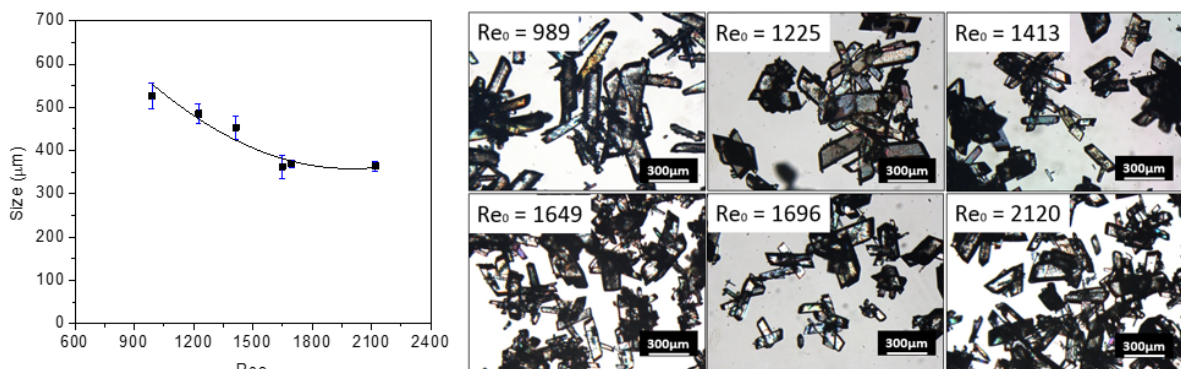
Figure 6. (Left) the effect of oscillatory Reynolds number on crystals size from COBR-1 to COBR-6; (right) images of crystal products taken from COBR-1 to COBR-6 under different mixing intensities

3.4 Steady state and crystal properties

For a batch crystallization process, the entire batch is cooled from a starting to an end temperature in a temporal domain. For a continuous process, however a very small fraction of solution is passing through pre-set temperature zones in a spatial domain; solution concentrations and crystal sizes measured at two different locations along the COBR enable the determination of spatial steady states, the rate of supersaturation consumption and local crystal growth rate. Solution concentrations and crystal sizes measured at different times in the same location in COBR allows the determination of temporal steady states. In this work, samples were taken at three sampling points of C1-C3 along the COBR at seed loading of 15 % as shown in Figure 2 and these concentration profiles as a function of time are displayed in Figure 7. Firstly, the concentration decreased from C1 to C3, verifying the correct operational path. Secondly the temporal steady states of concentration C1, C2 and C3 are clearly seen in Figure 7 where the difference in concentrations over different times is very small. Note that there is a tiny time delay at the start for C3 compared to C2 due to its location away from the feeding point. The spatial steady states of concentration can be assessed by the differences between C1 and C2, C1 and C3, C2 and C3, have also been achieved due to constant difference over time.
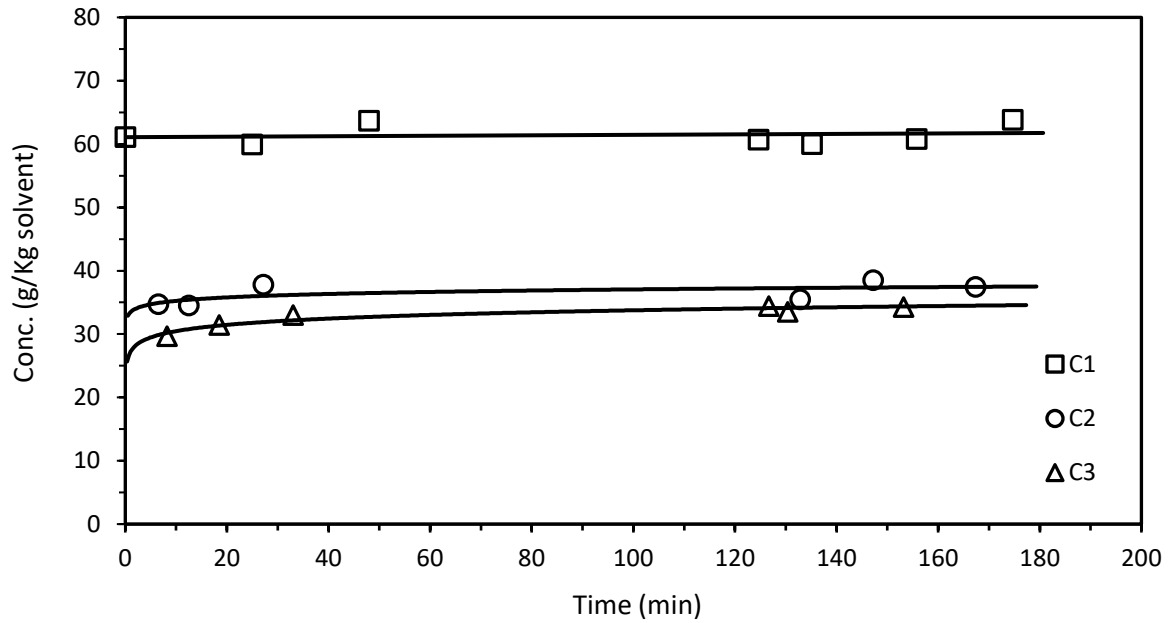
Figure 7. Concentration profile of C1-C3 in the COBR at 15 % seed loading. Trend lines show the temporal steady state of solute concentration, constant distances between trend lines indicate the spatial steady state
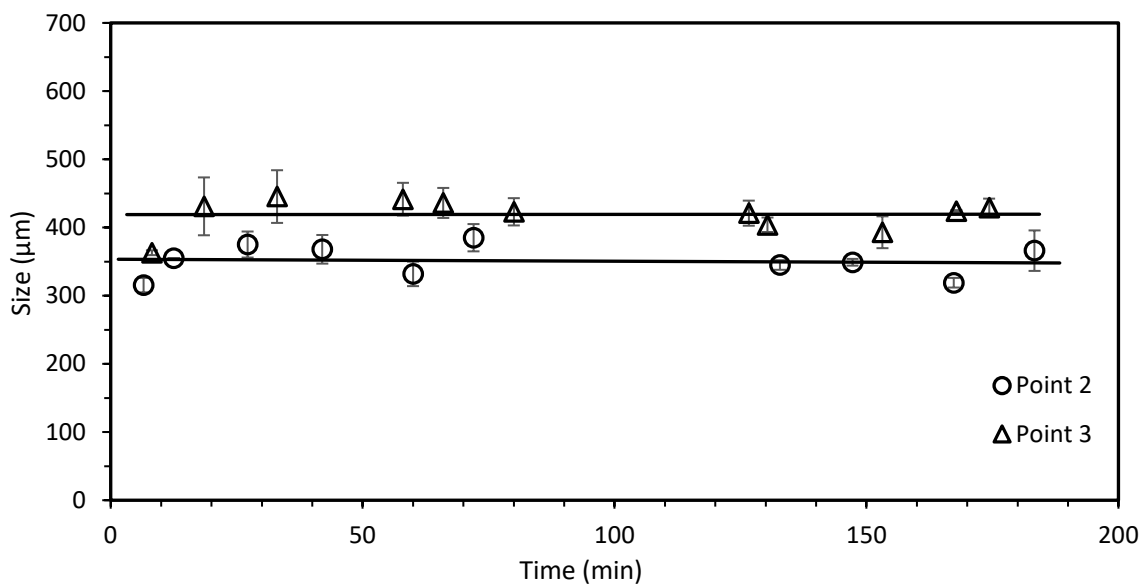

Figure 8. Size measurement for particles taken at sample point 2 and 3 at 15 % seed loading, trend lines show the temporal steady state of crystal size, constant distance between trend lines illustrates the spatial steady state.

Figure 8 shows the profile of mean particle sizes over time at sampling points 2 & 3. Crystal sizes increase from 350.95 μm at point 2 to 419.17 μm at point 3 extracted from SEM images in Figure 9. The temporal steady state was generally achieved with small fluctuations observed for particle sizes over time. Similarly, Brown et al.[6] reported both temporal and spatial steady states for solute concentrations in an anti-solvent crystallization of salicylic acid in a COBR, however, the temporal steady state for crystal size was unattainable due to the unstable flow rates, while spatial steady state in crystal size was obtained.

The constant increase in crystals size between the two locations denotes that the spatial steady state was attained. Given a fixed distance of 1.7 m and the flow rate of 50 g min^{-1}, the local crystal growth rate between the two locations is calculated as 1.89×10^{-7} m s^{-1} for the supersaturation ratio of 1.10. This is comparable with previous literatures on paracetamol growth kinetics. [25, 26, 39, 60] If we assume a linear relationship between supersaturation and crystal growth,[51] the overall growth rate would be 3.14×10^{-7} m s^{-1} for the global supersaturation of 1.82 in this work. Although the level of supersaturation is a bit higher than previous studies, the growth rate is comparable with results of Mitchell et al.[26] and Worlitschek[57] of paracetamol in ethanol. The crystal growth rate for a reactive unseeded cooling crystallization of paracetamol in a batch OBR was 4.30×10^{-7} m s^{-1} under a similar supersaturation (S=1.91), [49] the higher value for the unseeded process indicates less control over crystal growth rates. An overall growth rate of 6.36×10^{-7} m s^{-1} was reported for antisolvent crystallization of paracetamol, which is also higher than our data of cooling crystallisation.[61]

By assuming that the local growth rate is fully fueled by the consumption of the driving force (supersaturation), [51] the growth rate constant, k, was evaluated as 5.74×10^{-5} kg m^{-2} s^{-1}, which is lower than 3.7×10^{-4} kg m^{-2} s^{-1} for the reactive unseeded crystallization of paracetamol in an OBR.[49] This is likely attributed to the utilization of seeds for controlling the growth rate.
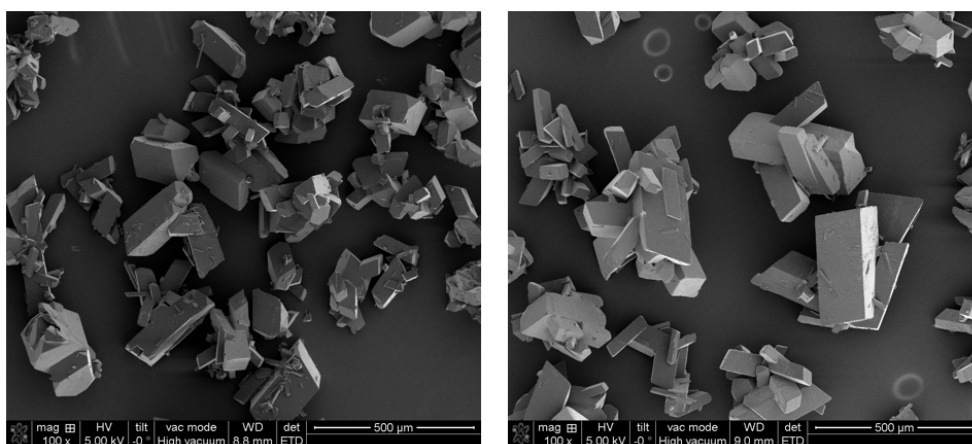
Figure 9. SEM images for particles taken at sample point 2 (left) and 3 (right) at 15 % seed loading, showing crystals growth along COBR

In general, SEM images of crystal products in the COBR in Figure 9 display elongated column shapes, which is the same as that in an OBR at the same solvent composition.[49] The XRD results (Figure 10) indicate that the polymorphism of paracetamol products in this work is of the sable Form I, which agrees with literature works.[33, 62]
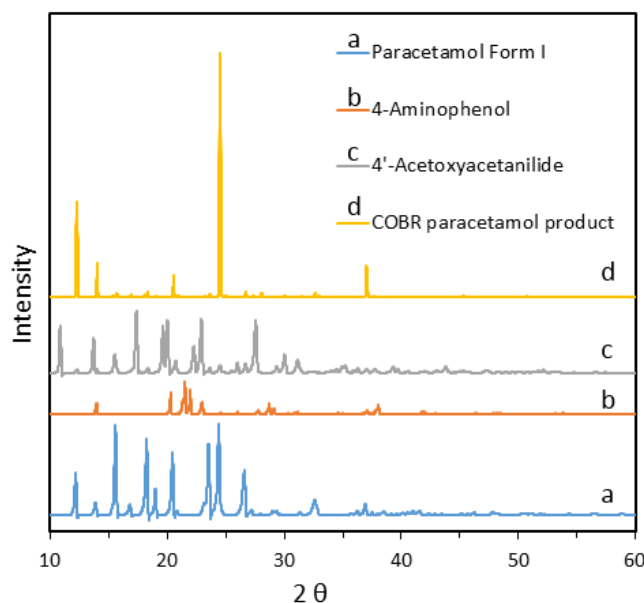

Figure 10. PXRD data for representative paracetamol particles produced in this work as well as purchased paracetamol (Form I) and possible impurities of 4-aminophenol and 4'-acetoxyacetanilide from previous study[48]

Crystals obtained from COBR were analyzed by HPLC, giving an average purity of 99.96% from 8 samples taken at sample point 3.

4 Conclusions

We report, for the first time, a reactive seeded cooling crystallization of paracetamol successfully performed in a COBR. We investigated the seeding strategy of three seed masses (10, 15, and 20 %) at a fixed size in this work, enabling smooth and encrustation free runs with the crystallization path close to the solubility curve. We also discussed crystal agglomeration by comparing the ideal to actual normalized product sizes. The effect of mixing intensity on crystal properties was discussed, crystals size reduced with the increase of R_{eo} number. By analyzing the concentrations and crystal sizes at two locations along the COBR, both temporal and spatial steady states in concentration and size were attained. The local growth rate was found to be 1.89×10^{-7} m s^{-1} when crystals flowed from point 2 to point 3, with the predicted overall growth rate as 3.73×10^{-7} m s^{-1} for a global supersaturation of 1.82. Crystals of polymorphic form I were continuously generated with an average purity of 99.96 %.

Acknowledgements

Nomenclature

c	Concentration in solution, kg $_{solute}$ kg^{-1} $_{solvent}$
c*	Solubility data at the same temperature, kg $_{solute}$ kg^{-1} $_{solvent}$
C_{seed}	Seed loading, %
D	Diameter of column, mm
F	Crystal shape factor constant

F_{main}	Main flow rate, g min^{-1}
F_{seed}	Flow rate for seeding solution, g min^{-1}
N	Number of seed crystals
Re_n	Net flow Reynolds number
Re_o	Oscillatory Reynolds number
S	Supersaturation ratio
S_{ip}	Ideal size of product crystals, μm
S_p	Actual products size, μm
S_s	Size of seed crystals, μm
St	Strouhal number
W_{seed}	Mass of seed crystal, g
W_{theo}	Mass of dissolved solute turned into crystals, g

Greek letters

ρ_s	Density of solid crystal, g ml^{-1}

Abbreviations

4-AP	4-aminophenol
AA	Acetic anhydride
C1	Concentration of paracetamol in solution at sample point 1
C2	Concentration of paracetamol in solution at sample point 2
C3	Concentration of paracetamol in solution at sample point 3
COBR/COBC	Continuous oscillatory baffled reactor
MSZW	Metastable zone width
OBR/OBC	Oscillatory baffled reactor
STC	Stirred tank crystallizer

References

(1)   Ni, X.; Fitch, A.; Laird, I., Mixing apparatus and process. US Patent 9295955, 2016.

(2)   Ni, X, Method and apparatus for phase separated synthesis. US Patent 6429268, 2002.

(3)   McGlone, T.; Briggs, N. E.; Clark, C. A.; Brown, C. J.; Sefcik, J.; Florence, A. J. *Org. Process Res. Dev.* **2015,** *19*, 1186-1202.

(4)   Lawton, S.; Steele, G.; Shering, P.; Zhao, L.; Laird, I.; Ni, X. *Org. Process Res. Dev.* **2009,** *13*, 1357-1363.

(5)   Briggs, N. E.; Schacht, U.; Raval, V.; McGlone, T.; Sefcik, J.; Florence, A. J. *Org. Process Res. Dev.* **2015,** *19*, 1903-1911.

(6)   Brown, C. J.; Adelakun, J. A.; Ni, X. *Chem. Eng. Process.* **2015,** *97*, 180-186.

(7)   Zhao, L.; Raval, V.; Briggs, N. E.; Bhardwaj, R. M.; McGlone, T.; Oswald, I. D.; Florence, A. J. *CrystEngComm* **2014,** *16*, 5769-5780.

(8)   Morse, H. *Ber. Dtsch. Chem. Ges.* **1878,** *11*, 232-233.

(9)   Davenport, K. G.; Hilton, C. B., Process for producing N-acyl-hydroxy aromatic amines. US Patent 4524217A, 1985.

(10)   Fritch, J. R.; Fruchey, O. S.; Horlenko, T.; Aguilar, D. A.; Hilton, C. B.; Snyder, P. S.; Seeliger, W. J., Production of acetaminophen. US Patent 5155273, 1992.

(11)   Ghiaci, M.; Aghaei, H.; Oroojeni, M.; Aghabarari, B.; Rives, V.; Vicente, M.; Sobrados, I.; Sanz, J. *Catal. Commun.* **2009,** *10*, 1486-1492.

(12)   Bassford, J. H. H., Manufacture of hydroxy amino compounds. US Patent 2132454, 1938.

(13)   Henke, C. O.; Vaughen, J. V., Reduction of aryl nitro compounds. US Patent 2198249, 1940.

(14)   Louis, S., Manufacture of aromatic parahydroxyamines. US Patent 2765342, 1956.

(15)   Godfrey, W.; De, A. J., Process of preparing nu-acetyl-p-amino phenol. US Patent 2998450, 1961.

(16)   Rode, C.; Vaidya, M.; Chaudhari, R. *Org. Process Res. Dev.* **1999,** *3*, 465-470.

(17)   Tingle, J. B.; Williams, L. F. *J. Am. Chem. Soc.* **1907,** *37*, 51.

(18)   Duesel, B. F.; Godfrey, W., Process for the preparation of n-acetyl-p-aminophenol (apap). US Patent 3341587, 1967.

(19)   Van Ness, J. H.; Warner, J. B., Preparation of N-acetyl-p-aminophenol. US Patent 4670589, 1987.

(20)   Young, D. W., Preparation of N-acetyl-p-aminophenol. US Patent 3113150, 1963.

(21)   Baron, F. A.; Schulman, H. L.; Weinberg, A. E., Preparation of N-acetyl-p-aminophenol. US Patent 3917695A, 1975.

(22)   Ellis, F., *Paracetamol: a curriculum resource*. Royal Society of Chemistry: London, 2002.

(23)   Lee, T.; Lin, H. Y.; Lee, H. L. *Org. Process Res. Dev.* **2013,** *17*, 1168-1178.

(24)   Lee, H. L.; Lin, H. Y.; Lee, T. *Org. Process Res. Dev.* **2014,** *18*, 539-545.

(25)   Ó'Ciardhá, C.; Mitchell, N.; Hutton, K.; Frawley, P. *Ind. Eng. Chem. Res.* **2012,** *51*, 4731-4740.

(26)   Mitchell, N. A.; Ó'Ciardhá, C. T.; Frawley, P. J. *J. Cryst. Growth* **2011,** *328*, 39-49.

(27)   Fujiwara, M.; Chow, P. S.; Ma, D. L.; Braatz, R. D. *Cryst. Growth Des.* **2002,** *2*, 363-370.

(28)   Reis, N. M.; Liu, Z. K.; Reis, C. M.; Mackley, M. R. *Cryst. Growth Des.* **2014,** *14*, 3191-3198.

(29)   Mitchell, N. A.; Frawley, P. J. *J. Cryst. Growth* **2010,** *312*, 2740-2746.

(30)   Acevedo, D.; Tandy, Y.; Nagy, Z. K. *Ind. Eng. Chem. Res.* **2015,** *54*, 2156-2166.

(31)   Ristic, R.; Finnie, S.; Sheen, D.; Sherwood, J. *JPCB* **2001,** *105*, 9057-9066.

(32)   Powell, K. A.; Saleemi, A. N.; Rielly, C. D.; Nagy, Z. K. *Chem. Eng. Process.* **2015,** *97*, 195-212.

(33)   Méndez del Río, J. R.; Rousseau, R. W. *Cryst. Growth Des.* **2006,** *6*, 1407-1414.

(34)   Brown, C. J.; Ni, X.-W. *Cryst. Growth Des.* **2011,** *11*, 3994-4000.

(35)   Brown, C. J.; Ni, X.-W. *CrystEngComm* **2012,** *14*, 2944-2949.

(36)   Brown, C. J.; Ni, X. *Cryst. Growth Des.* **2011,** *11*, 719-725.

(37)   Fusaro, F.; Mazzotti, M.; Muhrer, G. *Cryst. Growth Des.* **2004,** *4*, 881-889.

(38)   Kachrimanis, K.; Malamataris, S. *J. Pharm. Pharmacol.* **1999,** *51*, 1219-1227.

(39)   Granberg, R. A.; Bloch, D. G.; Rasmuson, Å. C. *J. Cryst. Growth* **1999,** *198*, 1287-1293.

(40)   Granberg, R. A.; Rasmuson, Å. C. *J. Chem. Eng. Data* **1999,** *44*, 1391-1395.

(41)   Yu, Z. Q.; Chow, P. S.; Tan, R. B. *Org. Process Res. Dev.* **2006,** *10*, 717-722.

(42)   Hermanto, M. W.; Chow, P. S.; Tan, R. B. *Ind. Eng.Chem.Res.* **2012,** *51*, 13773-13783.

(43)   Agnew, L. R.; McGlone, T.; Wheatcroft, H. P.; Robertson, A.; Parsons, A. R.; Wilson, C. C. *Cryst. Growth Des.* **2017,** *17*, 2418-2427.

(44)   Agnew, L. R.; Cruickshank, D. L.; McGlone, T.; Wilson, C. C. *Chem. Commun.* **2016,** *52*, 7368-7371.

(45)   Stonestreet, P.; Van Der Veeken, P. *Chem. Eng. Res.Des.***1999,** *77*, 671-684.

(46)   Ni, X.; Gough, P. *Chem. Eng. Sci.* **1997,** *52*, 3209-3212.

(47)   Mackley, M.; Stonestreet, P. *Chem. Eng. Sci.* **1995,** *50*, 2211-2224.

(48)   Jiang, M.; Ni, X. *Chem. Eng. Process.* **2018,** *131*, 20-26.

(49)   Jiang, M.; Ni, X. *Ind. Eng. Chem. Res.* **2018,** submitted.

(50)   Eder, R. J.-P.; Schmitt, E. K.; Grill, J.; Radl, S.; Gruber-Woelfler, H.; Khinast, J. G. *Cryst. Res. Technol.* **2011,** *46*, 227-237.

(51)   Mullin, J. W., *Crystallization*. Butterworth-Heinemann: Oxford, 2001.

(52)   Kubota, N.; Onosawa, M. *J. Cryst. Growth* **2009,** *311*, 4525-4529.

(53)   Doki, N.; Kubota, N.; Sato, A.; Yokota, M.; Hamada, O.; Masumi, F. *AlChE J.* **1999,** *45*, 2527-2533.

(54)   Narducci, O.; Jones, A.; Kougoulos, E. *Org. Process Res. Dev.* **2011,** *15*, 974-980.

(55)   Beckmann, W. *Org. Process Res. Dev.* **2000,** *4*, 372-383.

(56)   Davey, R.; Garside, J., *From molecules to crystallizers*. Oxford University Press: New York, 2000.

(57)   Ni, X.; Liao, A. *Chem. Eng. J.* **2010,** *156*, 226-233.

(58)   Hamzah, A. A.; Hasan, N.; Takriff, M. S.; Kamarudin, S. K.; Abdullah, J.; Tan, I. M.; Sern, W. K. *Chem. Eng. Res. Des.* **2012,** *90*, 1038-1044.

(59)   Pereira, N. E.; Ni, X. *Chem. Eng. Sci.* **2001,** *56*, 735-739.

(60)   Worlitschek, J.; Mazzotti, M. *Cryst. Growth Des.* **2004,** *4*, 891-903.

(61)   Brown, C. J.; Ni, X. *Cryst. Growth Des.* **2011,** *11*, 719-725.

(62)   Barthe, S. C.; Grover, M. A.; Rousseau, R. W. *Cryst. Growth Des.* **2008,** *8*, 3316-3322.